The Influence of the Particle Size Distribution on Fluidized Bed Hydrodynamics Using High-Throughput Experimentation

Renske Beetstra and John Nijenhuis
Delft University of Technology–DelftChemTech, 2628 BL Delft, The Netherlands

Naoko Ellis
Delft University of Technology–DelftChemTech, 2628 BL Delft, The Netherlands; and
Dept. of Chemical and Biological Engineering, University of British Columbia, Vancouver, BC, Canada V6T 1Z3

J. Ruud van Ommen
Delft University of Technology–DelftChemTech, 2628 BL Delft, The Netherlands

DOI 10.1002/aic.11790
Published online June 16, 2009 in Wiley InterScience (www.interscience.wiley.com).

The goal of the described project is to design mixtures of particles with optimal fluidization properties. Using high-throughput experimentation, a novel approach to study hydrodynamics in fluidized beds, the relevant properties can be obtained in a limited period of time. This approach is demonstrated by assessing the influence of particle size distribution on fluidized bed hydrodynamics of Geldart A powders. By manipulating the width of the particle size distribution of alumina powder, the bubble diameter is reduced up to 40%. The addition of fines to a given particle size distribution also decreases the bubble diameter up to 40%, whereas the addition of coarse particles hardly influences the bubble size. At low gas velocities, the bubble size was found to increase with fines addition or increasing standard deviation. © 2009 American Institute of Chemical Engineers *AIChE J,* 55: 2013–2023, 2009
Keywords: particle size distribution, bubble size, fluidization, fines

Introduction

The two main reactor types for catalyzed gas phase reactions are packed bed and fluidized bed. In packed beds, the catalyst particles are normally no smaller than 1 mm to prevent excessive pressure drop. This leads to mass transfer limitations within the particles. Fluidized beds do not suffer from this drawback: small particles (typically 20–400 μm) can be used while the pressure drop stays low. It is expected that catalyst efficiency will increase strongly in the coming years because of the increased possibilities of molecular modeling, the use of high-throughput techniques in catalysis engineering, and the advances in synthesis methods.[1–3] This will make the mass transfer problems in packed beds even more severe. Thus, a shift from packed beds to fluidized beds or structured reactors based on thin catalyst layers can be expected in the process industry within the next decade. Although fluidized beds do not suffer from mass transfer limitations on the particle scale, they have mass transfer limitations on a larger scale: the transport from gas in the dilute phase (voids or bubbles) to the particles in the dense phase. Consequently, the conversion of reactant(s) in the dilute phase is much lower than in the dense phase. This leads to a low overall conversion, since for fluidized beds of small particles, the dilute phase conversion dictates the overall conversion. Figure 1 shows the effect of bubble size on the conversion in

Correspondence concerning this article should be addressed to J. Ruud van Ommen at j.r.vanommen@tudelft.nl.

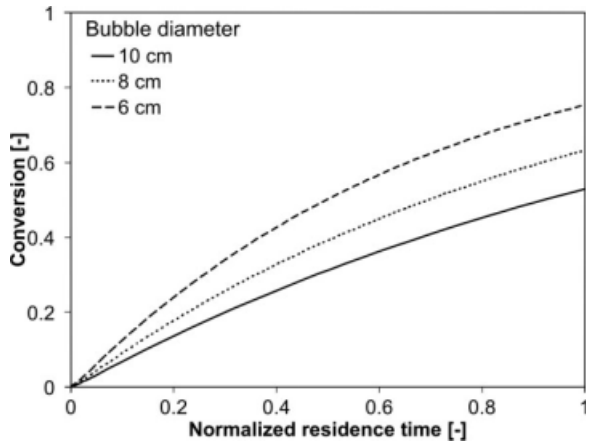

Figure 1. The effect of bubble size on the conversion of reactant(s) in a fluidized bed, based on the Kunii and Levenspiel model.[4]

The legend shows the bubble diameters used in the calculation.

a fluidized bed for an arbitrary (mass transfer limited) first-order reaction, calculated with the Kunii and Levenspiel model.[4] In this case, the conversion increases from 53% to 75% when the bubble diameter is decreased from 10 cm to 6 cm. If we could do this in practice, the recycling of unreacted material could be decreased by almost half.

A reduction of bubble size or an increase in the particle content of the bubbles will lead to a smaller difference in conversion between the dilute and dense phases and a higher overall conversion. Moreover, in the case of reactions in parallel or in series (the most realistic situations), the narrower residence time distribution resulting from a lower concentration difference between the phases leads to a higher selectivity for the desired product. In the past, our group has studied three different ways to introduce structure in fluidized beds to reduce the bubble size[5]: oscillating the gas supply, distributing the gas supply over the height of the bed, and varying the interparticle forces using electric fields. In addition to these approaches, we have recently initiated a study to increase the efficiency of fluidized beds by optimizing the particle size distribution (PSD). Compared with the other methods of improving fluidized bed performance, this approach has the advantage that, in principle, no modifications to the fluidized bed equipment are necessary.[6]

It is a well-known fact in fluidization technology that the addition of fines (particles with a diameter <45 μm[7]) improves the fluidization behavior and leads to a better mass transfer. The underlying mechanism, however, has never been fully explained; although, it has often been speculated that fines act as a kind of lubricant to lower the apparent viscosity of the dense phase, leading to smaller voids and more uniform gas-solid distribution. Sun and Grace[8] have shown experimentally that a wider PSD leads to a higher conversion for ozone decomposition. They suggested that this effect was due to an increased amount of fines in the dilute phase compared with the dense phase.[9]

The current practice is, however, that particles for fluidized beds (carriers for catalytic material) are optimized with a focus on their catalytic activity rather than hydrodynamic behavior of the bed. Most attention is given to their pore size distribution such that a high surface area is achieved and that the active sites are easily accessible by gaseous reactants. Consequently, very little attention is paid to the mass transfer from the gas in the dilute phase to the particles in the dense phase, which is essential for practical fluid bed operation. Therefore, this work is aimed at improving the conversion and selectivity of gas–solid fluidized reactors by designing mixtures of particles with an optimal size distribution with the aid of high-throughput experimentation, a novel approach for hydrodynamic research.

It is desirable to have experimental data for all relevant variables over a wide range at a high resolution, to find trends and optimum values in fluidization characteristics. Furthermore, considerable variance in measured data is expected due to the dynamic behavior of the fluidized bed itself. Therefore, to distinguish between the results and to find an ''optimal'' value for a property (e.g., fraction of fine particles of a given size), all main input variables need to be controlled and measured at high accuracy. Examples of these input variables are temperature, flow rate, pressure, relative humidity, bed mass, and composition. This, in combination with the need of testing a large number of particle mixtures, leads to the need for high-throughput experimentation approach. An additional advantage is that no direct human interaction is needed due to the fully automated character of this high-throughput experimentation. Furthermore, more dangerous materials could be tested safely under a wide range of conditions. Examples are nanoparticles and particles coated with nanomaterials such as those used in pharmaceutics.

Experimental

3D high-throughput setup

To obtain quantitative information from large numbers of bed material, an automated setup was constructed. The operating procedure of the setup is schematically depicted in Figure 2. It is possible to load and empty the fluidized bed column with selected particle mixtures (of e.g. sand or catalyst carrier materials such as silica or alumina) fully automatically. The loading of this mixture in the fluidized bed column is handled by a Zymark XP Robot (see Figure 3). The column is emptied by blowing the particles out with a very high gas flow rate.

The experiments were conducted in a stainless steel column of 40 cm high with an internal diameter of 7.3 cm.

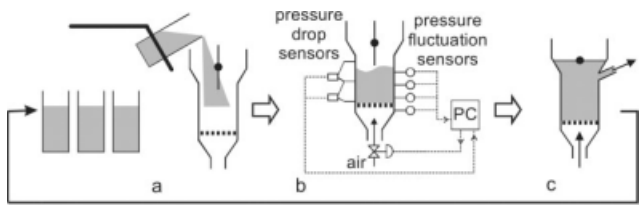

Figure 2. Schematic representation of the high-throughput screening procedure.

a. Filling the fluidized-bed column; b. Carrying out the measurement program; c. Emptying the column. After c, the whole procedure is automatically repeated with the next batch of particles.

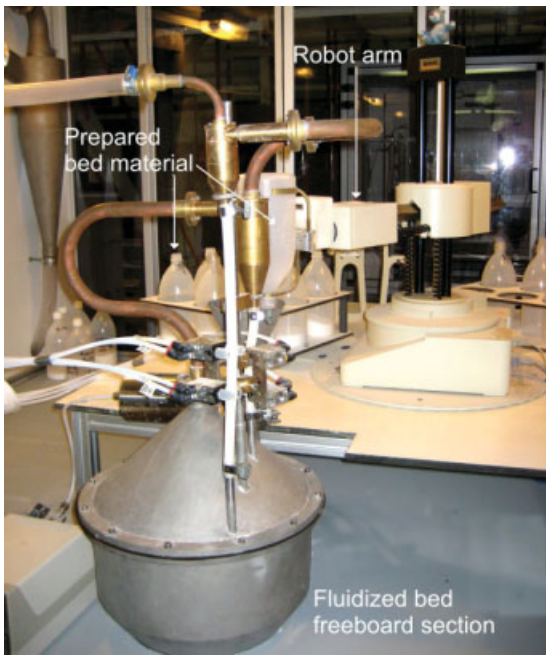

Figure 3. Loading of a bed mass with the Zymark XP robot.

[Color figure can be viewed in the online issue, which is available at www.interscience.wiley.com.]

An expanded section is placed above the column with a diameter of 35 cm. To ensure constant conditions during experiments, temperature and humidity are controlled. Three mass flow controllers controlled the airflow through the fluidized bed with maximum superficial velocities of 0.008, 0.08, and 0.8 m/s, respectively. The gas is distributed through a porous plate (Sika-R3) of the same diameter as the column, with a thickness of 3 mm. The experiments can be carried out in two industrially relevant fluidization regimes: bubbling fluidization and turbulent fluidization. Two cyclones are installed at the gas outlet to recycle particles that elutriated from the column.

To illustrate the novel concept of using high-throughput experimentation techniques to determine the effect of particle size and PSD on the fluidization behavior, four types of experiments were conducted with porous alumina powder ($\rho_s = 1300$ kg/m^3):

- *Experiment A:* The effect of fines (i.e., particles $< 45\mu$m) on the bubble size was examined by studying the hydrodynamic behavior of bed material consisting of a mixture of base particles with a median particle size (D_{50}) of 70 μm and fines ($D < 45$ μm). The fines weight fraction is varied from 0 to 50 wt %.
- *Experiment B:* The influence of fines on the hydrodynamic behavior of base particles of different sizes was studied. The base particles had sizes varying from 70 to 118 μm. Twenty weight percent fines were added to these base particles, while the bubble sizes in the mixtures and the corresponding bed masses of only base particles were compared.
- *Experiment C:* The effect of broadening the PSD on the fluidization hydrodynamics is investigated by varying the standard deviation of the PSD in seven steps from 40 to 188 μm, while D_{50} is kept constant at 172 μm.
- *Experiment D:* Twenty weight percent secondary particles of various sizes were added to base particles with a D_{50} of 70 and 172 μm. To the base particles with a D_{50} of 70 μm, we added 20% alumina powder with a D_{50} of 23, 49, 58, 70, 83, 98, 115, 138, 172, or 195 μm, respectively. To the base particles with a D_{50} of 172 μm, we added 20% with a D_{50} of 23, 49, 58, 83, 115, 172, 217, 265, 328, or 425 μm, respectively. From the results of this experiment, it can be derived if bubble size reduction is caused by fines exclusively or if any variation of the PSD (even adding larger particles) has similar effects.

For all experiments, a mass of 0.50 kg particles was used, resulting in packed bed heights around 15 cm. Superficial gas velocities were varied from 0.02 to 0.24 m/s (minimum fluidization velocities were 2.8×10^{-3} m/s for the 70 μm base particles and 7.7×10^{-3} m/s for the 172 μm particles; for the mixtures they ranged from 2 to 8×10^{-3} m/s). Table 1 gives an overview of the base particle properties.

In the experiments, two types of pressure measurements are acquired to assess the hydrodynamics. First, the pressure drop over parts of the bed is measured to determine the average bed density and the bed expansion, which is a measure for the total amount of gas in the bed. The pressure drops were measured with two Validyne DP15 pressure transducers. Second, high-frequency pressure fluctuations were measured in the plenum, and at 7 and 14 cm above the distributor plate, with probes 10 cm long and an internal diameter of 4 mm. These dimensions ensure minimum disturbance to the signals in the frequency range of interest.[10] All probes were purged with air at 0.5 m/s to prevent blocking.

The pressure fluctuations were measured with Kistler piezoelectric pressure sensors (type 7261). All signals were low-pass filtered with a cutoff frequency of one half of the sample frequency, satisfying the Nyquist criterion. Subsequently, 16-bit analogue to digital conversion was applied at a sample frequency of 400 Hz. A recently developed spectral decomposition method[11] enabled us to determine the bubble size from these pressure fluctuation measurements. This technique separates the part of the pressure time-series that is directly related to bubbles passing the pressure sensor from pressure fluctuations that are measured through the entire bed, including the plenum. The bubble size is calculated from the standard deviation in the incoherent (local) pressure fluctuations $\sigma_{xy,i}$:

$$D_b \sim \frac{\sigma_{xy,i}}{\rho_s g(1-\varepsilon_{mf})} \tag{1}$$

where ρ_s is the solids density and ε_{mf} is the porosity at minimum fluidization. The absolute bubble diameter cannot be determined from Eq. (1). However, based on this equation, bubble sizes in systems with similar solids can be compared and a relative bubble size can be calculated.

Table 1. Particle Properties Used in this Research

Powder ID	70 μm	85 μm	172 μm	Fines
D_{10} (μm)	56.6	68.1	145	5.8
D_{50} (μm)	69.9	85.5	172	31.1
D_{90} (μm)	85.2	107	212	49.8
$D_{3,2}$ (μm)	68.2	83.4	173	11.5
U_{mf} (10^{-3} m/s)	2.8	4.8	7.7	–

The porosity at minimum fluidization that is used in Eq. (1) is determined from the bed expansion at minimum fluidization. The pressure drop in the bed is measured in two stages: the lower stage measures the pressure drop between a height of 0 and 7 cm in the column and the higher stage measures the pressure drop between 7 and 35 cm. Assuming that the solids distribution is homogeneous throughout the bed, the bed height is calculated with Eq. (2):

$$H = 7.0 \times \frac{(\Delta P_{0-7} + \Delta P_{7-35})}{\Delta P_{0-7}} (\text{cm}) \tag{2}$$

The porosity at minimum fluidization is calculated from the bed height, the total mass in the bed, and the solids density.

Two optical probes of 6 mm in diameter were installed in the column, at $h = 14$ and 16 cm. The probes are inserted 2.0 cm inside the column, which is based on the findings of Werther and Molerus (cited in Levenspiel[12]) and our experimental experience. This insertion length ensures the registration of bubbles, because an increase in signal amplitude was noticed when the probe was inserted for more than 1 cm into the bed. Influence on the fluidization hydrodynamics due to the probes is assumed to be reduced in comparison with an insertion length of half the column diameter. Data is recorded with a sampling rate of 400 Hz, which results in a reasonable boundary for the detectable bubble velocity of 8 m/s. A drop in the signal strength of an optical probe indicates the passage of a bubble. The signals from the two probes are processed in Matlab. The average bubble rise velocity is determined from the sum of squares method, giving an estimate for the time lag between the two signals. To find the peaks in the two signals that are caused by the same bubble, a window around this average is studied. The time lag between the passage of a bubble at the lower probe and the upper probe gives us the rise velocity of a specific bubble. The bubble size can then be estimated from the time of the signal change and this rise velocity. Obviously, this is not always the maximum diameter of a bubble as it may pass the optical probe on the side. However, this effect will be the same for all bed compositions, and therefore, these data can be used to determine the relative bubble sizes. The matching of signals from the two probes is not always ideal: in some cases, a bubble does not move vertically, or it coalesces or changes shape with a different signal at the second probe as a consequence. If there is no matching signal found in the studied time frame, the peak is rejected. A peak is also rejected when the signal change is not large enough with respect to the dense phase.

Pseudo-2D setup

Although the high-throughput setup provides data on the bubble size, it is not possible to actually see the bubbles. Therefore, additional experiments were performed in a pseudo-2D column for video analysis. The column width and depth are 20.9 cm by 1.54 cm. It was filled to a height of around 15 cm with similar alumina particles as used in the 3D column. The gas distributor is a porous plate, similar to the 3D setup. Temperature and humidity of the fluidizing air are controlled, as is the flow rate. An Olympus i-speed 2 camera at 200 and 400 fps with a 2 Gb internal memory recorded the bed behavior. A light was placed behind the fluidized bed to make bubbles appear as lighter spots that can be recognized by video analysis software. The resolution of the camera is 800 $\times$ 600 pixels. Calibration of the bubble sizes was done from markings on the column. The bubble diameter is given as the size of the lighter area that is recognized as a "bubble" by the software. The bed materials used in these experiments were base particles of $D_{50} =$ 85 μm, and the same base particles with 20 wt % fines. The minimum fluidization velocity of these particles is measured at 4.8 $\times$ 10^{-3} m/s.

Results and Discussion

Minimum fluidization velocities and porosities

The minimum fluidization velocities were determined from the total pressure drop over the bed. Figure 4a shows an example for the base particle mixture ($D_{50} = 70$ μm). Figure 4b shows the measured bed heights for the same experiment, determined from the pressure drop at two different locations as shown in Eq. (2). The height at minimum fluidization was determined by extrapolating the trend line of the heights in the fluidized state of the bed (above U_{mf}), as indicated in the figure. The extrapolation method was

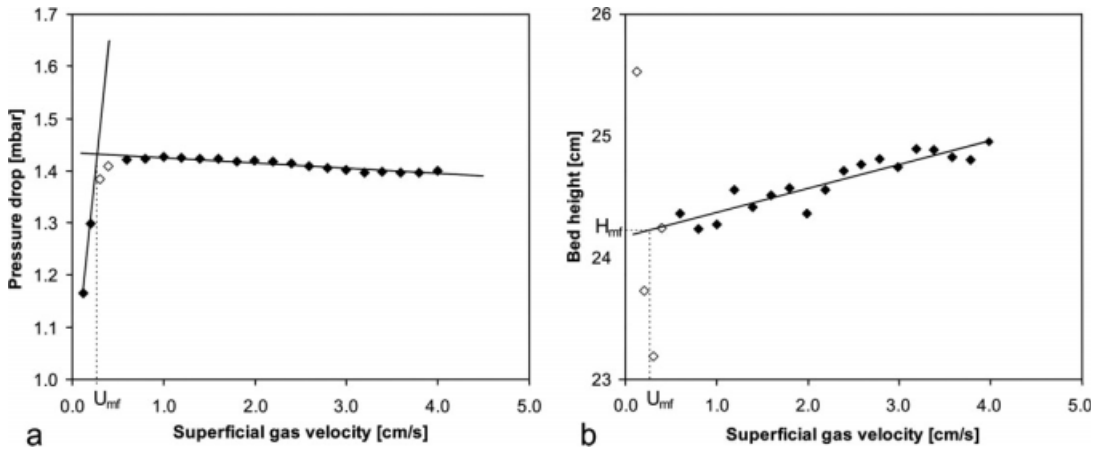

Figure 4. Determination of minimum fluidization velocity (a) and bed height at minimum fluidization (b).

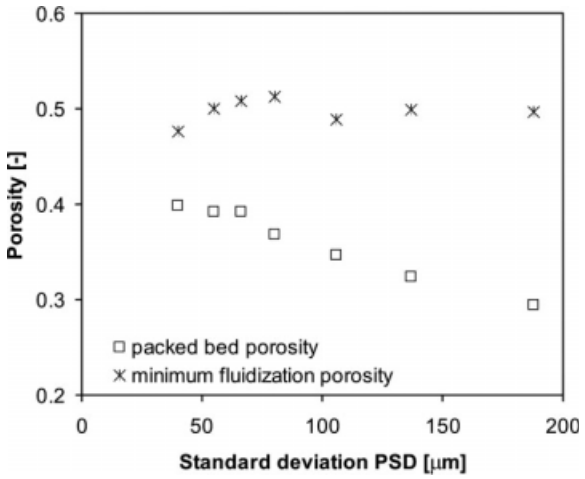

Figure 5. Porosity at minimum fluidization and (dense) packed bed porosity as a function of standard deviation of the particle size distribution for mixtures with D_{50} = 172 μm.

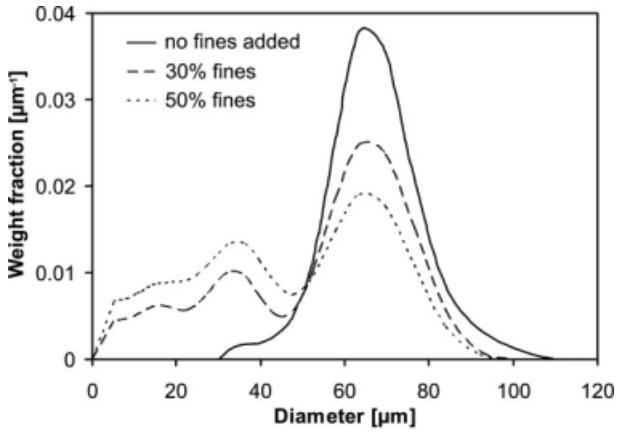

Figure 6. Three of the particle size distributions used in Experiment A.

Base particles: $D_{50} = 70$ μm.

chosen, because it was found that the measured heights at and below U_{mf} fluctuated strongly. This can be seen from the four points at the lowest velocities in Figure 4b. The determination of the height by measuring the pressure drop is probably not reliable enough when the bed is not moving freely.

Figure 5 shows the minimum fluidization porosities for the mixtures with $D_{50} = 172$ μm, used in Experiment B, as a function of the standard deviation of PSD. The porosity is almost constant at $\varepsilon = 0.5$. Contrary to this, the packed bed porosity decreases with increasing standard deviation. The data that are indicated by the squares in Figure 5 are the dense-packed bed porosities: the bed was tapped several times before measuring the porosity. There is thus considerable bed expansion from packed bed to a bed at minimum fluidization conditions.

Experiment A

To investigate the effect of adding fines on the fluidization behavior, the fines concentration was varied from 0 to 50 wt %. Figure 6 shows three of the resulting PSDs.

In these experiments, the relative bubble size was calculated by spectral decomposition of the measured pressure fluctuations and plotted as a function of the fines weight fraction. Figure 7a shows the relative bubble sizes (normalized with the bubble size in a bed without fines) at a height of 7 cm in the bed with increasing addition of fines. The bubble diameters decrease up to 55%. Furthermore, a strong dependence on the superficial gas velocities is shown. At the lowest velocity of 0.02 m/s, the bubble size even increases with the addition of fines. Figure 7b shows the same data at a height of 14 cm in the bed. The graph is very similar; however, the increase in bubble diameter at low velocities is even more pronounced here.

With respect to the dependency of the results on the gas velocity, it is important to notice that Sun and Grace[8] observed the largest effect on conversion for higher

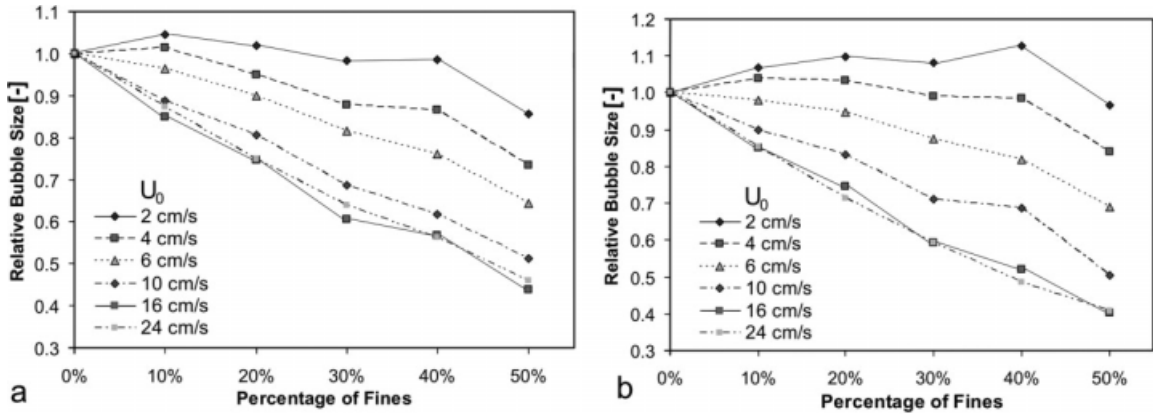

Figure 7. Relative bubble size (normalized by bubble size for a mixture without fines at the same velocity) based on pressure fluctuation measurement as a function of fines weight fraction at varying superficial gas velocities.

a. $h = 7$ cm; b. $h = 14$ cm.

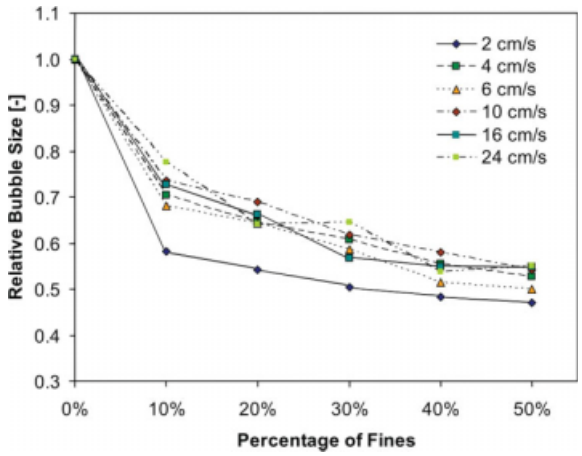

Figure 8. Relative bubble size based on optical probe measurement as a function of fines weight fraction at varying U_0.

[Color figure can be viewed in the online issue, which is available at www.interscience.wiley.com.]

velocities (0.3–1.3 m/s). Yates and Newton[7] found a lower conversion with higher gas velocities (they measured from 0.06 to 0.33 m/s), but no conclusion is drawn with respect to the influence of fines as a function of gas velocity. Sun and Grace[9] found a strong effect on the solids concentration in voids for higher velocities ($U > 0.4$ m/s) as well. None of the authors mentioned here performed experiments at a velocity lower than 0.06 m/s. Therefore, they did not notice any reverse effects for low velocities.

Optical probe measurements have shown a decrease in relative bubble size with increasing fines content in the bed material, as is shown in Figure 8. However, optical probe measurements did not indicate an increase in bubble size at low velocities. The difference may be due to the small size of bubbles: the chance of a small bubble passing the tip of the optical probe is much smaller than for a larger bubble. A small bubble might move around the obstacle, leaving only the larger bubbles to be detected by the optical probes. Furthermore, when a small bubble passes the tip of the probe, the "interface" is not far from the probe tip and might reflect some light. When this happens, the analysis program might reject the bubble because the threshold value to recognize a bubble is not reached. The correlation of two optical probe signals was indeed lower for the 0.02 m/s experiments, and fewer bubbles were observed. Another possible explanation for the different results from optical probes in the 0.02 m/s case is that the bubble shape changes: a flat bubble would seem to have a smaller diameter in an optical probe measurement, whereas it does not influence the pressure measurements.

It should be noted that, in some experiments at higher gas velocities, very large average bubble sizes were measured by the optical probes, and in some experiments even larger than the column diameter. A closer inspection of the raw data indicated that bubbles were often passing the probes in groups. When the signal does not return to the threshold value in between the passage of two bubbles, these might be seen as one larger bubble. Changing the threshold value could improve this; however, this would also imply that fewer bubbles are detected. We decided to keep the threshold constant to make a fair comparison between the various experiments.

Several authors have reported increased conversion of chemical reactions in a fluidized bed with higher fines contents[7,8,13]; it is often assumed that this is due to bubble size reduction. In our experiments, we have demonstrated the direct relation between the fines content and this bubble size reduction at industrially relevant gas velocities, which is a first step in finding the fundamental mechanism behind this phenomenon. However, at lower gas velocities, the bubble sizes increased with fines content.

Experiment B

Figure 9a shows the effect of 20 wt % fines addition on the relative bubble size with varying base particle sizes (average diameters of the base particles are given in the

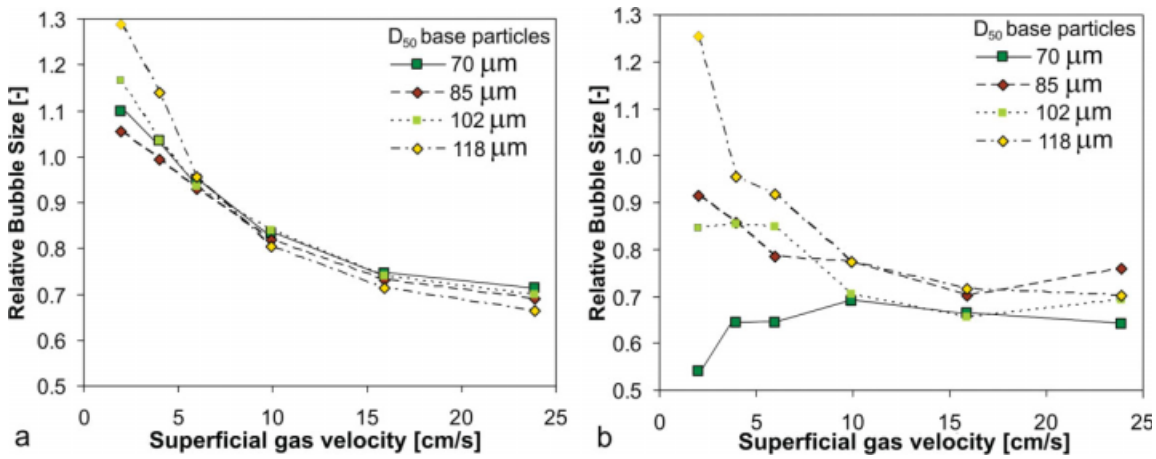

Figure 9. Relative bubble size in a mixture with 20 wt % fines as a function of gas velocity for different base particle sizes. The legends show the average base particle diameter in micrometers.

a. From pressure fluctuation measurements; b. From optical probes. [Color figure can be viewed in the online issue, which is available at www.interscience.wiley.com.]

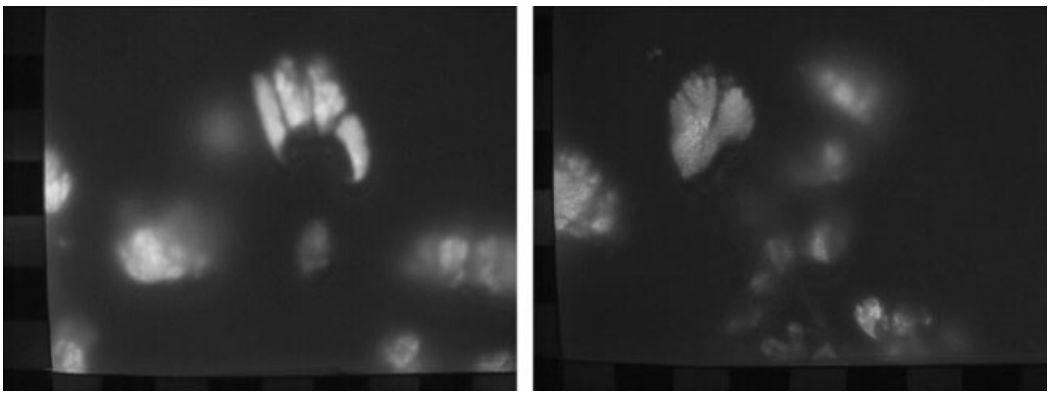

Figure 10. Snapshots from the pseudo 2D experiments.

Images taken from the experiments at $10U_{mf}$ or 0.048 m/s. Left: base particles, $D_{50} = 85$ μm. Right: base particles + 20 wt % fines.

legend of the figure). All bubble sizes for the mixtures are relative to a bed mass with the base particles at the same gas velocity. The relative bubble sizes are comparable in all systems, showing that the effect is not limited to the base particles used in Experiment A. The results from the optical probes, shown in Figure 9b, show reasonable agreement for the higher velocities and for the largest base particles. For the smaller particles, there is a difference at lower fluidization velocities similar to the observations in Experiment A.

The bed masses consisting of base particles of $D_{50} = 85$ μm and $D_{50} = 85$ μm with 20 wt % fines were also used in the pseudo 2D setup. Experiments were done at three different velocities: 7.1×10^{-3} m/s ($1.5U_{mf}$), 0.048 m/s ($10U_{mf}$), and 0.095 m/s ($20U_{mf}$). Snapshots from the experiments at 0.048 m/s are shown in Figure 10. Bubble size histograms obtained from video analysis of around 500 bubbles for each experiment are shown in Figure 11. They confirm what was observed in the 3D experiments using pressure fluctuation measurements: at low velocities, an increase in bubble diameter is observed, whereas at higher velocities, the bubble size clearly decreases. Table 2 shows the average diameters calculated from the bubble analysis and the relative average bubble diameter in the case when fines are added (normalized with the case without fines at the same velocity). The average diameter is calculated from the averaged projected area. Comparing the 0.095 m/s 2D experiment to the 0.10 m/s 3D experiment (see Figure 9) shows that the relative bubble diameter is slightly lower in the 2D case. In the $U_0 = 0.048$ m/s measurement, the 2D result for relative bubble size is much lower than the 0.04 m/s case in the 3D setup. The 7.1×10^{-3} m/s experiments cannot be compared directly to a 3D measurement since those were not performed at such low velocities. However, these experiments confirm the increasing bubble size at low velocities. In fact, the relative bubble diameter observed in this experiment is higher than in any of the 3D experiments. It is likely that the effect of increasing bubble size when fines are added becomes stronger closer to the minimum fluidization velocity of the mixture.

Care should be taken in interpreting the 2D data. The depth of the bed might be limiting, especially for larger bubbles. If a bubble cannot grow in depth, it might become wider or higher resulting in larger projected area. On the other hand, some bubbles are too small to reach through the entire bed depth and, as a result, not as bright as full depth bubbles on the images. Therefore, some of the images might

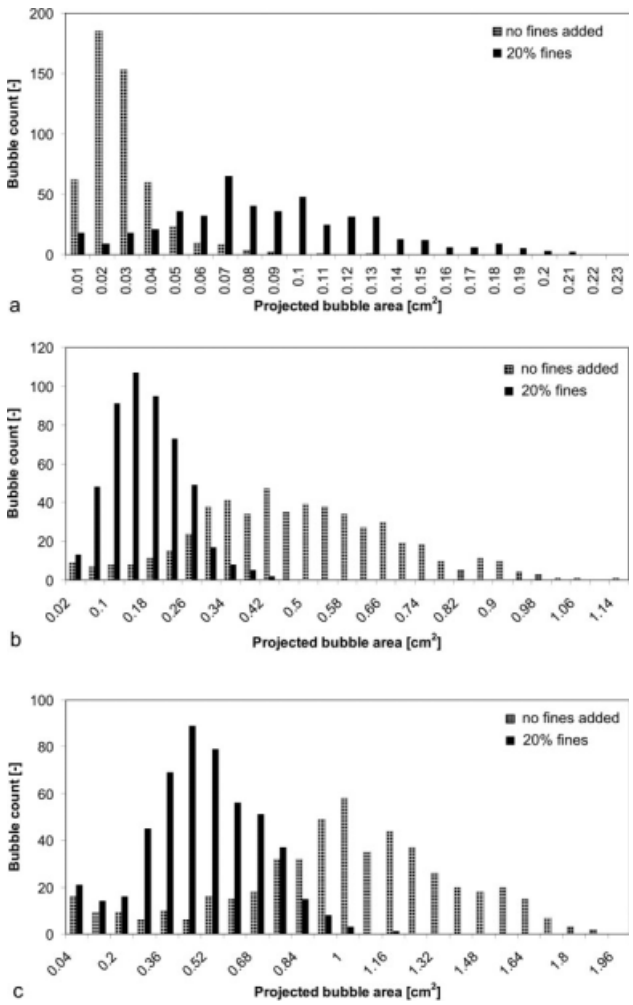

Figure 11. Bubble size distributions in pseudo 2D bed using video analysis.

a. $U_0 = 7.1 \times 10^{-3}$ m/s ($1.5U_{mf}$); b. $U_0 = 0.048$ m/s ($10U_{mf}$); c. $U_0 = 0.095$ m/s ($20U_{mf}$).

Table 2. Average Bubble Sizes Observed in the Pseudo 2D Experiment

Velocity (10^{-3} m/s)	Average Bubble Diameter (cm)		Relative Average Bubble Diameter with Fines
	No Fines	20% Fines	
7.1 ($1.5U_{mf}$)	0.172	0.325	1.89
48 ($10U_{mf}$)	0.778	0.459	0.590
95 ($20U_{mf}$)	1.121	0.786	0.701

not be recognized by the software as bubbles or as smaller bubbles only. This can also be seen in the snapshots in Figure 10. Another issue in the video analysis is the raining of particles through the bubbles. If the solids holdup in the bubble is very high, this has a similar effect as a bubble that does not cover the complete depth: a bubble might not be recognized at all, or as a smaller bubble, or be broken into smaller bubbles by the analysing software. The raining seemed to be stronger in the experiments with fines (see Figure 10).

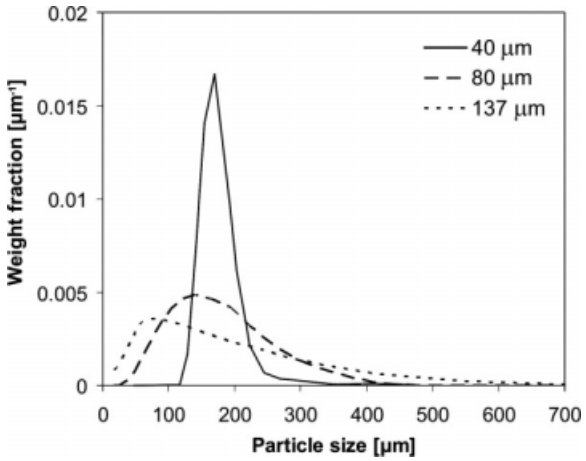

Figure 12. Some of the particle size distributions with D_{50} = 172 μm and varying standard deviation used in Experiment B.

The legend shows the standard deviation of the distribution.

Experiment C

Figure 12 shows some of PSDs that were used in Experiment C. The PSD broadens with constant median particle size (D_{50} = 172 μm) by addition of smaller and larger particles. Sun and Grace[8] demonstrated that a wider PSD results in higher conversions than obtained by narrow distributions. The bubble size reduction induced by changing the standard deviation of the PSD was measured as a function of the gas velocity. Spectral decomposition of the measured pressure fluctuations revealed that the bubble size decreases significantly while increasing the standard deviation of the PSD (see Figure 13a). The effect becomes stronger at higher gas velocity. At the lowest gas velocity, an increase in bubble diameters is indicated again. Data are further supported by the results obtained by the optical probes (see Figure 13b), even for the increase in bubble size in the 0.02 m/s experiment, as opposed to Experiment A, where the increasing diameter was not observed with the optical probes. A possible explanation is the fact that in this experiment larger base particles are used, resulting in a larger bubble size, which is better detected by our system.

Experiment D

Experiment D was designed to reveal the influence of adding fine or coarse particles to a base material on fluidization behavior. Ten fractions of particles with different D_{50} were added one by one (20 wt %) to the base powder with a D_{50} of 70 μm. The same was done for the base particles of 172 μm. Figure 14 shows the relative bubble sizes as a function of the median diameter (D_{50}) of the added fraction. The bubble sizes are normalized with the bubble size in a fluidized bed of only the base particles at the same superficial

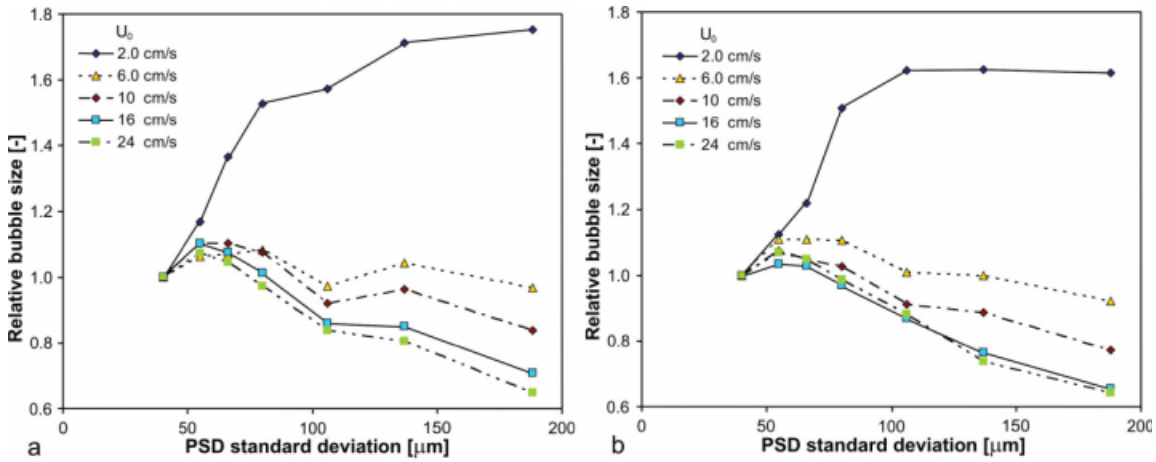

Figure 13. Relative bubble size as a function of the standard deviation of PSD for various U_0 (specified in the legend).

The median diameter in all cases was close to 172 μm. a. Bubble sizes determined from pressure fluctuations at h = 14 cm; b. Optical probe measurements at h = 14 cm. [Color figure can be viewed in the online issue, which is available at www.interscience.wiley.com.]

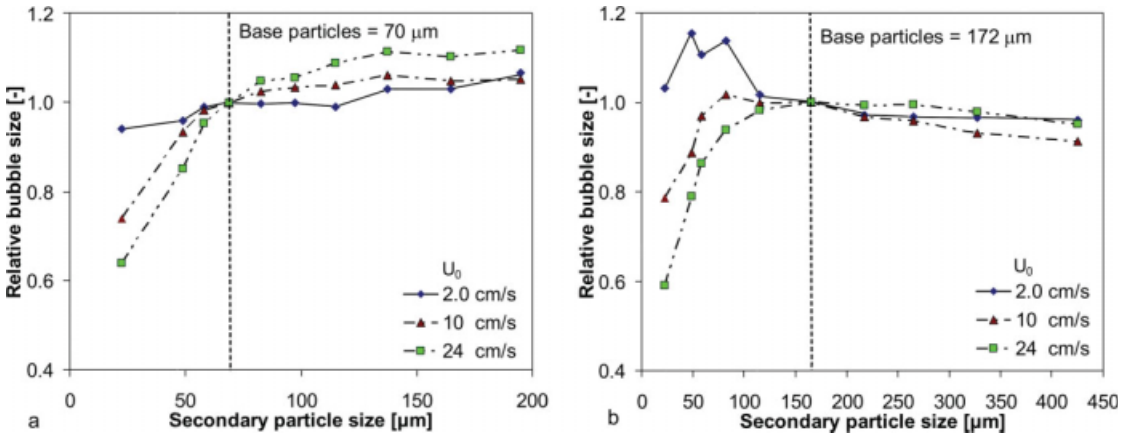

Figure 14. Relative bubble sizes as a function of the secondary particle size for various U_0 (specified in the legend).

Bubble sizes determined from pressure fluctuations at $h = 14$ cm, normalized with the bubble size in a mixture of only base particles. Twenty weight percent secondary particles were added to the base particles. Median base particle diameters: a. $D_{50} = 70$ μm; b. $D_{50} = 172$ μm. [Color figure can be viewed in the online issue, which is available at www.interscience.wiley.com.]

gas velocity. These results show that smaller particles affect the fluidization hydrodynamics to a much greater extent than larger particles for both base particle sizes.

In general, the results show a large influence of PSD on the hydrodynamic behavior of a fluidized bed. The presence of fines influences the bubble size strongly. However, at low gas velocities the bubble size increases, whereas it decreases with fines content at higher velocities. Moreover, the results illustrate that it is very helpful to have proper tools to conduct a large set of experiments with changing PSD with high precision and in a limited period of time.

Mechanism

As mentioned earlier, the mechanism underlying the decrease in bubble size with the addition of fines is not yet fully understood. The possibility of a decrease of the granular viscosity, because of a lubricating effect of the fines, was proposed in literature. However, it seems that a decrease of granular viscosity (if this indeed occurs) is a symptom rather than an explanation. In the kinetic theory of granular flow,[14] the granular viscosity μ_s is calculated from:

$$\mu_s = \frac{\theta_s}{2n_s}\sum_{n=1}^{NP}\left(1+\frac{8\pi}{15}\sum_{p=1}^{NP} n_p D_{np}^3 M_{pn}\frac{1+e_{np}}{2}g_{np}\right)n_n b_0^{(n)} + \frac{4}{15}\sqrt{2\pi\theta_s}\sum_{n=1}^{NP}\sum_{p=1}^{NP} n_n n_p D_{np}^4\sqrt{m_n M_{pn}}\frac{1+e_{np}}{2}g_{np} \quad (3)$$

In Eq. (3), μ_s is the solid phase viscosity, θ_s the granular temperature, n_i the particle number density for species i and n_s the total particle number density, NP the number of solid phases, D_{ij} the sum of radii of particles i and j, m_i the mass of particle i and M_{ij} the reduced mass. b_0 is a Sonine coefficient from the Enskog approximation of the kinetic theory. The restitution coefficient for a collision between particles i and j is represented by e_{ij} and g_{ij} is the radial distribution function for a mixture. This can be derived from the radial distribution function for a single component g_0 by Eq. (4):

$$g_{np}(\varepsilon_s, x_1, ..., x_{NP-1}, D_1, ..., D_{NP}) = \frac{1}{1-\varepsilon_s} + \left[g_0(\varepsilon_s) - \frac{1}{1-\varepsilon_s}\right]\frac{\langle D^{(2)}\rangle D_n D_p}{\langle D^{(3)}\rangle D_{np}} \quad (4)$$

$$g_0(\varepsilon_s) = 1 + 4\varepsilon_s\frac{1+2.5000\varepsilon_s+4.5904\varepsilon_s^2+4.515439\varepsilon_s^3}{\left[1-\left(\frac{\varepsilon_s}{\varepsilon_s^{max}}\right)^3\right]^{0.67802}} \quad (5)$$

with x_i the number fraction of particles of species i, where we took the radial distribution function of Ma and Ahmadi[15] for g_0 in Eq. (5). Note that in Eq. (4) it is not taken into account that the maximum packing density changes for a mixture of different sized particles. However, this is especially important at high packing densities, close to the maximum density [which is assumed to be 0.64356 in Eq. (5)]. For our calculations in a fluidized bed of fine particles we used $\varepsilon = 0.5$.

When we use Eq. 3 to calculate the granular viscosity in a mixture, keeping all parameters except the PSD the same, an increase in viscosity is found when fines are added (see Figure 15). This is probably due to the increased number of particles and therefore increased number of collisions in the mixture. When the binary mixture is compared to monodisperse particles with the same Sauter mean diameter, a slight decrease of viscosity is visible, but the change does not seem to be large enough to have the effect on the bubble size that was seen in the experiments. If there is indeed a change in the granular viscosity, it is more likely that it has a different cause, e.g. a change in dense phase porosity or granular temperature (particle velocity distribution). However, it seems to be a side effect rather than the main cause for the decrease in bubble size.

Sun and Grace[8] noticed that the solids holdup in the dilute phase is higher when fines are added to the bed. This can explain a higher conversion when a wide or bimodal PSD is used. However, it is not the full explanation for the higher conversion, since inert fines also had a positive effect on the

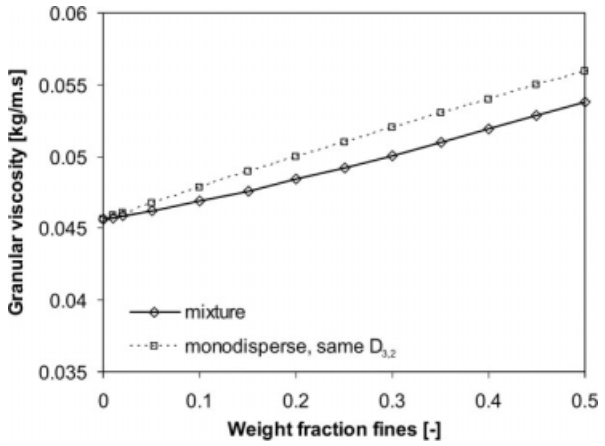

Figure 15. Granular viscosity in a binary mixture with varying fines fraction calculated with the kinetic theory of granular flow.[14]

conversion. It is likely that the decreased bubble size plays a part here.

A decrease in bubble size could also be explained from a lower amount of gas in the dilute phase, i.e., a higher gas flow through the dense phase. Yates and Newton[7] argue that the gas velocity in the dense phase increases with fines content. A higher porosity would also lead to a higher gas flow through the dense phase. This could be checked from collapse experiments. Collapse experiments by Khoe et al.[16] showed that, in mixtures with similar mean diameters, the dense phase porosity is lower at a higher fines content. However, similar collapse tests performed by Kono et al.[17] showed an increase of dense phase porosity with fines content. In the latter case, the fines consisted of a different material than the main particles and were much smaller than in the first case. This could influence the hydrodynamic behavior when van der Waals forces or electrostatic charging play a role. Thus, literature is not conclusive on the effect of fines on the dense phase porosity. In the Kunii and Levenspiel model,[4] it is assumed that the dense phase is always at minimum fluidization conditions ($U_{dense} = U_{mf}$; $\varepsilon_{dense} = \varepsilon_{mf}$). We noticed in our experiments that the minimum fluidization velocities decreased with higher fines content. This agrees with the findings of Cheung et al.,[18] who saw a strong influence on the minimum fluidization velocity when a small amount of fines was added. The measured porosities increase slightly at higher fines content, although the error is rather high in these experiments due to the way of determining the bed height. Apart from that, the assumption of minimum fluidization conditions for the dense phase in itself is questionable, especially for Geldart type A powders, with a large zone of homogeneous expansion between U_{mf} and U_{mb}. The data of Khoe et al.[16] suggest that assuming minimum fluidization conditions for the dense phase is reasonable at high gas velocities. At velocities up to about three times the minimum bubbling fluidization U_{mb}, the expansion of the dense phase is significant. Kono et al.[17] do not give values for minimum fluidization velocities and porosities of their mixtures, but a similar peak in the porosity around U_{mb} is observed (moreover, they define U_{mb} as the velocity at which the highest dense phase porosity is achieved). The decrease in porosity after U_{mb} seems to be smaller for mixtures when compared with the pure component in their results. Foscolo et al.[19] find that the dense phase porosity lies between the values for minimum fluidization and minimum bubbling porosities. They found values of ~0.8–0.85 times the minimum bubbling porosity.

Another aspect that could influence the bubble size is a difference in coalescence and break-up behavior. Sun and Grace[9] observed higher solids holdup in voids when fines are present. Since fines have a lower terminal velocity, it is expected that their residence time in a bubble is longer. In our 2D experiments, we have also noticed more solids raining though the bubbles in the case with fines. Perhaps, this raining initiates breakup of the voids. If fines are not distributed evenly over the dense phase, i.e. concentrated in the bubble wake or cloud, the fines holdup of the voids might be enhanced even more.

It is very likely that there is no single explanation for the effect that fines have on the hydrodynamic behavior of a fluidized bed, and in particular, the bubble size. The deviant behavior at low velocities is an indication that in fact two or more effects may be counteracting each other: a bubble-stabilizing effect prevailing at low velocities, and a bubble size decreasing effect dominating at higher velocities. In the near future, we will use a discrete particle model to gain more insight into the mechanisms that play a role. This type of models can give information on the processes on a particle scale.[20,21] Various interparticle forces like van der Waals forces and collision properties are expected to influence the bed behavior.

Conclusions

The use and potential of a novel high-throughput experimentation test facility for fluidization research has been demonstrated by assessing the influence of PSD on fluidized bed hydrodynamics. With this approach, the relevant fluidization properties can be obtained for a wide range of PSDs in a limited period of time. Bubble sizes were measured in two ways: using pressure fluctuations and optical probes.

By manipulating the width of the PSD of alumina powder, the bubble size can be reduced up to 40%. The addition of fines to a given PSD also decreases the bubble size up to 40%, whereas the addition of coarse particles hardly influences the bubble size. An opposing effect was seen at low gas velocities: bubble diameters increased rather than decreased with fines content. However, this last phenomenon was not observed with the optical probes in all experiments.

Experiments in a pseudo 2D column were analyzed using video. The results agreed reasonably well with the 3D experiments, showing increasing bubble diameters for the lowest gas velocity and decreasing diameters for higher velocities.

These data show that by optimizing particle mixtures, mass transfer from dilute phase to dense phase in fluidized beds can be improved. When this is taken into account when designing or optimizing industrial reactors, it may lead to considerable savings.

Acknowledgments

R. Monna is gratefully acknowledged for his skilful help in developing the setup. R. van Dijk and A. Leonardi-Romero performed many of the experiments. We want to thank the Dutch National Science Foundation, NWO, for their financial support.

Notation

$b_0^{(i)}$ = Sonine coefficient
D = (particle) diameter [m]
D_b = bubble diameter [m]
D_{10} = 10% of particles is smaller than this diameter [m]
D_{50} = median particle diameter [m]
D_{90} = 90% of particles is smaller than this diameter [m]
$D_{3,2}$ = surface-volume averaged particle diameter [m]
g = gravity constant [m/s^2]
g_0 = radial distribution function
g_{ij} = radial distribution function for mixture
h = height above distributor plate [m]
H_{mf} = bed height at minimum fluidization [m]
m = particle mass [kg]
M_{np} = reduced mass
n_i = number of particles of type i per unit volume [m^{-3}]
n_s = total number of particles per unit volume [m^{-3}]
ΔP = pressure drop [Pa]
U_{mb} = minimum bubbling velocity [m/s]
U_{mf} = minimum fluidization velocity [m/s]
U_0 = fluidization velocity [m/s]
x_i = number fraction of species i
ε = porosity
ε_s = solids volume fraction ($=1-\varepsilon$)
θ_s = granular temperature [kg m^2/s^2]
μ_s = solid phase viscosity [kg/(m s)]
ρ_s = particle density [kg/m^3]
$\sigma_{xy,i}$ = standard deviation in the incoherent pressure fluctuations [Pa]

Literature Cited

1. Broadbelt LJ, Snurr RQ. Applications of molecular modeling in heterogeneous catalysis research. *Appl Catalysis A*. 2000;200:23–46.
2. Senkan S. Combinatorial heterogeneous catalysis—a new path in an old field. *Angew Chem Int Ed*. 2001;40:312–329.
3. Ying JY, Mehnert CP, Wong MS. Synthesis and applications of supramolecular-templated mesoporous materials. *Angew Chem Int Ed*. 1999;38:56–77.
4. Kunii D, Levenspiel O. *Fluidization Engineering*, 2nd ed. Stoneham, MA: Butterworth-Heinemann, 1991:289–292.
5. Coppens M-O, Van Ommen JR. Structuring chaotic fluidized beds. *Chem Eng J*. 2003;96:117–124.
6. Van Ommen JR, Nijenhuis J, Van den Bleek CM, Coppens M-O. Four ways to introduce structure in fluidized bed reactors. *Ind Eng Chem Res*. 2007;46:4236–4244.
7. Yates JG, Newton D. Fine particle effects in a fluidized-bed reactor. *Chem Eng Sci*. 1986;41:801–806.
8. Sun G, Grace JR. The effect of particle size distribution on the performance of a catalytic fluidized bed reactor. *Chem Eng Sci*. 1990;45:2187–2194.
9. Sun G, Grace JR. Experimental determination of particle dispersion in voids in a fluidized bed. *Powder Techn*. 1994;80:29–34.
10. Van Ommen JR, Schouten JC, Vander Stappen MLM, Van den Bleek CM. Response characteristics of probe-transducer systems for pressure measurements in gas-solid fluidized beds: how to prevent pitfalls in dynamic pressure measurements. *Powder Techn*. 1999; 106:199–218; erratum: *Powder Techn*. 2000;113:217.
11. Van der Schaaf J, Schouten JC, Johnson F, Van den Bleek CM. Non-intrusive determination of bubble and slug length scales in fluidized beds by decomposition of the power spectral density of pressure time series. *Int J Multiphase Flow*. 2002;28:865–880.
12. Levenspiel O. *Chemical Reaction Engineering*, *3rd ed*. Chichester: Wiley, 1999.
13. Pell M, Jordan SP. Effect of fines and velocity on fluid bed performance. *AIChE Symp Ser*. 1988;262:68–73.
14. Goldschmidt MJV. *Hydrodynamic Modelling of Fluidised Bed Spray Granulation*. Ph.D. thesis, University of Twente. Enschede: University of Twente Press, 2001. Available at http://doc.utwente.nl/36352/.
15. Ma D, Ahmadi G. An equation of state for dense rigid sphere gases. *J Chem Phys*. 1986;84:3449–3450.
16. Khoe GK, Ip TL, Grace JR. Rheological and fluidization behaviour of powders of different particle size distribution. *Powder Techn*. 1991;66:127–141.
17. Kono HO, Ells TS, Chiba S, Suzuki M, Morimoto E. Quantitative criteria for emulsion phase characterization and for the transition between particulate and bubbling fluidization. *Powder Techn*. 1987;52:69–76.
18. Cheung L, Nienow AW, Rowe PN. Minimum fluidisation velocity of a binary mixture of different sized particles. *Chem Eng Sci*. 1974;29:1301–1303.
19. Foscolo PU, Di Felice R, Gibilaro LG. An experimental study of the expansion characteristics of gas fluidized beds of fine catalysts. *Chem Eng Process*. 1987;22:69–78.
20. Van der Hoef MA, Van Sint Annaland M, Kuipers JAM. Computational fluid dynamics for dense gas-solid fluidized beds: a multi-scale modeling strategy. *China Particuology*. 2005;3:69–77.
21. Van Wachem BGM, Almstedt AE. Methods for multiphase computational fluid dynamics. *Chem Eng J*. 2003;96:81–980.

Manuscript received July 16, 2008, and revision received Nov. 13, 2008.